Alteration of N-glycome in diethylnitrosamine-induced hepatocellular carcinoma mice: a non-invasive monitoring tool for liver cancer: Alteration of N-glycome in DENA-induced hepato...

ARTICLE *in* LIVER INTERNATIONAL: OFFICIAL JOURNAL OF THE INTERNATIONAL ASSOCIATION FOR THE STUDY OF THE LIVER · SEPTEMBER 2010

Impact Factor: 4.85 · DOI: 10.1111/j.1478-3231.2010.02279.x

Liver INTERNATIONAL
OFFICIAL JOURNAL OF THE INTERNATIONAL ASSOCIATION FOR THE STUDY OF THE LIVER

Liver International ISSN 1478-3223

BASIC STUDIES

Alteration of *N*-glycome in diethylnitrosamine-induced hepatocellular carcinoma mice: a non-invasive monitoring tool for liver cancer

Xue-en Liu[1,2,3], Sylviane Dewaele[2,3], Valerie Vanhooren[2,3], Ye-Dong Fan[4], Ling Wang[1], Jacques Van Huysse[5], Hui Zhuang[1], Roland Contreras[2,3], Claude Libert[2,3] and Cuiying Chitty Chen[2,3]

1 Department of Microbiology, Peking University Health Science Center, Beijing, China
2 Department for Molecular Biomedical Research, VIB, Ghent University, Ghent, Belgium
3 Department of Biomedical Molecular Biology, Ghent University, Ghent, Belgium
4 Department of Surgery, Ghent University Hospital, Ghent, Belgium
5 Department of Pathology, Ghent University Hospital, Ghent, Belgium

Keywords
DENA – hepatocellular carcinoma (HCC) – marker – *N*-glycan

Abbreviations:
APTS, 8-amino-1,3,6-pyrenetrisulphonic acid; CCC, cholangiocellular carcinoma; DENA, diethylnitrosamine; DSA-FACE, DNA sequencer-assisted (DSA), fluorophore-assisted carbohydrate electrophoresis (FACE); Fut, fucosyltransferase; GlcNAc, β-linked *N*-acetylglucosamine; HCC, hepatocellular carcinoma; NA2, bigalacto, biantennary glycan; NA2F, bigalacto, core-α-1,6-fucosylated biantennary; NA3, trigalacto, tri-antennary; PNGase F, peptide *N*-glycosidase F; β4Gal-T, β1,4-galactosyltransferases.

Correspondence
Cuiying Chitty Chen, Department for Molecular Biomedical Research, VIB & Ghent University, Technologiepark 927, B-9052 Ghent, Belgium
Tel: +32 93 313 702
Fax: +32 93 313 609
e-mail: cuiying.chen@dmbr.ugent.be

Received 23 February 2010
Accepted 26 April 2010

DOI:10.1111/j.1478-3231.2010.02279.x

Abstract

Background and aims: There is a demand for serum markers that can routinely assess the progression of liver cancer. DENA (diethylnitrosamine), a hepatocarcinogen, is commonly used in an experimental mouse model to induce liver cancer that closely mimics a subclass of human hepatocellular carcinoma (HCC). However, blood monitoring of the progression of HCC in mouse model has not yet been achieved. In this report, we studied glycomics during the development of mouse HCC induced by DENA. *Methods:* Mouse HCC was induced by DENA. Serum *N*-glycans were profiled using the sequencer assisted–Fluorophore-assisted carbohydrate electrophoresis technique developed in our laboratory. Possible alteration in the transcription of genes relevant to the synthesis of the changed glycans was analysed by real-time polymerase chain reaction. *Results:* In comparison with the control mice that received the same volume of saline, a tri-antennary glycan (peak 8) and a biantennary glycan (peak 4) in serum total glycans of DENA mice increased gradually but significantly during progression of liver cancer, whereas a core-fucosylated biantennary glycan (peak 6) decreased. Expression of α-1,6-fucosyltransferase 8 (Fut8), which is responsible for core fucosylation, decreased in the liver of DENA mice compared with that of age-matched control mice. Likewise, the expression level of Mgat4a, which is responsible for tri-antennary, significantly increased in the liver of DENA mice ($P < 0.001$). *Conclusions:* The changes of *N*-glycan levels in the serum could be used as a biomarker to monitor the progress of HCC and to follow up the treatment of liver tumours in this DENA mouse model.

Diethylnitrosamine (DENA) is a hepatocarcinogen known to cause DNA ethylation and mutagenesis (1). It is commonly used to induce liver cancer in animal models, and in rodents, it induces tumours that closely mimic a subclass of human hepatocellular carcinoma (HCC) (2). However, blood monitoring of the progression of HCC in a mouse model has not yet been achieved.

Most serum *N*-linked glycoproteins are synthesized by the liver and B-lymphocytes. Any change in serum total *N*-glycans could reflect an alteration of liver or B-lymphocyte physiology. Because the sugar chains of glycoproteins are important for maintaining the ordered 'social behaviour' of differentiated cells in multicellular organisms, alterations in these sugar chains contribute to the molecular basis of abnormalities such as invasion of tumour cells into the surrounding tissues and their metastasis to distant sites/tumour cell invasion and metastasis. Several studies have linked changes in certain *N*-glycosylation patterns to human disease (3–7). Alterations in the *N*-linked sugar chains are indeed found in various tumours (8–11). Moreover, we and others recently showed that certain changes in the *N*-glycans in total serum protein are indicative of human HCC (8), non-alcoholic steatohepatitis (NASH) (9), liver fibrosis (10) and cirrhosis (11). These observations are in line with the fact that a large fraction of serum proteins are

produced by hepatocytes. Therefore, *N*-glycan changes in serum proteins are potential reporters of liver dysfunction.

Here, we show that serum *N*-glycan analysis by DNA sequencer assisted–fluorophore-assisted carbohydrate electrophoresis (DSA-FACE) can be used to evaluate the progression of liver HCC in mice treated with DENA.

Materials and methods

Animals and treatment

Three-week old female C57BL/6j mice with an average weight of 15.8 ± 1.5 g SD were purchased from Elevage Janvier (Le-Genest-Saint-Ile, France). All mice were housed in specific pathogen free animal facilities. They were maintained in a temperature-controlled, air-conditioned environment with 14–10-h light/dark cycles, and they received food and water *ad libitum*. Experimental protocols and procedures for the animal experiments were approved by the Ghent University Animal Ethics Committee, Belgium.

The mice were divided into two groups: a DENA-treated group and a control group starting from the age of 4 weeks. Mice in the DENA group were injected weekly with DENA (Sigma-Aldrich, St Louis, MO, USA) at 75 μg/g body weight (BW) for 3 weeks and then at 100 μg/g BW weekly for another 3 weeks intraperitoneally. At the same time, mice in the control group received the same volume of saline in the same scheme. Control mice and DENA mice were killed at different time points: 23, 30, 36 and 48 weeks after the initiation of DENA administration. Serum samples were collected to investigate serum *N*-glycan profiles. Mice were killed under anaesthesia, weighed and examined for the presence of visible lesions. The right lobe of the liver in control mice and the tumour in DENA mice were removed and fixed in 4% formalin for histology and pathology or snap-frozen in liquid nitrogen for RNA analysis.

Histology and pathology

Liver sections of 4 μm were cut from paraffin-embedded blocks and stained with haematoxylin and eosin (H&E), Masson's trichrome and reticulin for histological examination. Liver samples were evaluated independently by two experienced hepatopathologists who were not informed of the glycomics results.

Processing blood samples for protein *N*-glycome analysis

The *N*-glycans present on the proteins in 2 μl of serum were released, labelled and analysed by DSA-FACE as described previously (12, 13), with some minor modification. Briefly, 2 μl serum was added in a polymerase chain reaction (PCR) tube containing 2 μl of buffer (10 mM NH_4HCO_3, pH 8.3, 5% SDS) and 3 μl of water. The tube was heated at 95 °C for 5 min and cooled for 15 min at 4 °C in a PCR thermocycler. Then, 3 μl of peptide-*N*-glycosidase F (PNGase F) was added (2.2 U/μl in 10 mM NH_4HCO_3, pH 8.3, containing 3.33% NP40) (New England Biolabs, Hitchin, UK). The tubes were incubated in the thermocycler at 37 °C for 3 h, cooled to 4 °C and then 100 μl of water was added. Six microlitres of the resulting solution were transferred to a new PCR tube and evaporated to dryness at 60 °C in the thermocycler (lid open). *N*-glycans were derivatized by adding 1 μl of labelling solution [1:1 mixture of 20 mM 8-amino-1,3,6-pyrenetrisulphonic acid (APTS); Molecular Probes, Eugene, OR, USA] in 1.2 M citric acid and 1 M $NaCNBH_3$ in dimethyl sulphoxide). The tightly closed tubes were incubated at 37 °C for 16 h. The APTS labelling reaction was stopped by adding 200 μl of water. Then, 2 μl of APTS-labelled solution was transferred to a new PCR tube for digestion with 0.25 mU *Arthrobacter ureafaciens* sialidase (Roche, Mannheim, Germany) in 5 μl of 5 mM NH_4Ac, pH 5. The tube was incubated overnight at 37 °C in the thermocycler. Labelled *N*-glycans were analysed by DSA-FACE using a capillary electrophoresis (CE)-based ABI3130 sequencer (Applied Biosystems, Foster city, CA, USA). Data were analysed using the GeneMapper v3.7 software (Applied Biosystems). We measured the heights of the 10 peaks that were detected in all the samples to obtain a numerical description of the profiles.

For structural analysis of APTS-labelled serum *N*-glycans, appropriate amounts were digested with exoglycosidases: *Streptococcus pneumonia* β-1,4-galactosidase (0.4 mU/digest), jack bean β-*N*-acetylhexosaminidase (10 mU/digest), bovine kidney α-fucosidase (2 mU/digest) and almond meal α-1,3/4-fucosidase (1 μU/digest) (all from Prozyme, San Leandro, CA, USA). DSA-FACE was used to analyse the digestion products.

Statistical analysis

Statistical analyses were performed with SPSS 15.0 for Windows software (SPSS, Chicago, IL, USA). Results are presented as means ± SD. All reported *P*-values are two-tailed, using a *t*-test for independent samples.

RNA, cDNA and quantitative polymerase chain reaction

Thirty milligrams of frozen liver tissue was ground in liquid nitrogen and RNA was prepared with the RNeasy Mini Kit (Qiagen Benelux B.V., Venlo, the Netherlands). A DNase digestion was performed with the Qiagen RNase-Free DNase Set. For cDNA synthesis, 150 ng of random primers (Roche Diagnostics, Vilvoorde, Belgium) were allowed to anneal with 5 μg of total RNA in 12 μl Rnase-free water and then combined with 5 μl of 5 × reaction buffer (250 mM Tris-HCl, pH 8.3, 375 mM KCl, 15 mM $MgCl_2$), 2.5 μl 0.1 M DTT, 1.25 μl of 10 mM dNTPs (Roche Diagnostics), 20 U RNase Block (Stratagene, Huissen, the Netherlands) and 2.75 μl DEPC-H_2O. The mixture was incubated at room temperature for 2 min, combined with 200 U of Superscript II RT (Invitrogen, Merelbeke, Belgium) and incubated for 10 min at 25 °C and 50 min at 42 °C. The enzyme was inactivated at

70 °C for 15 min, and the RNA template was removed by incubation with 2 U of RNase H (1.5 U/μl; Promega, Benelux BV, Leiden, the Netherlands) at 37 °C for 20 min. The cDNA was stored at − 20 °C.

Real-time quantitative PCR (qPCR) using the Light Cycler 480 (Roche Diagnostics) was performed with a 16-fold dilution of the cDNA. Each 10-μl assay contained 5 μl of 2xLightCycler 480 SYBR Green I Mastermix (Roche Diagnostics) containing FastStart Taq DNA Polymerase, reaction buffer, dNTP mix (with dUTP instead of dTTP), SYBR Green I dye, $MgCl_2$, 1 μl primer mix for each gene (final concentration of 0.5 μM each) and 4 μl of diluted cDNA (Roche Diagnostics). The housekeeping genes RPL13a.1 and Hprt1 were used as a reference to normalize the liver sample data. Each reaction was performed in triplicate. PCR cycling consisted of denaturation at 95 °C for 5 min, 50 cycles of 95 °C for 10 s and 60 °C for 30 s, followed by detection for 1 s at 72 °C. The Ct data were analysed with Excel and GRAPHPAD PRISM 4 (GraphPad Software Inc. La Jolla, CA, USA). Primers were selected from the Primer Bank of Harvard (http://pga.mgh.harvard.edu/primerbank) and sequences are presented in Table 1.

Results

Diethylnitrosamine treatment induced cholangiocellular carcinoma and hepatocellular carcinoma

We induced liver tumours in C57BL/6j mice by injecting them intraperitoneally six times with the alkylating agent DENA starting at the age of 4 weeks and monitored weight and tumour development for 48 weeks. BW was significantly lower ($P < 0.05$) in the DENA-injected mice (23.03 ± 1.87 g; $n = 48$) compared with the control group (26.41 ± 1.37 g; $n = 34$). To monitor tumour development, the mice were sacrificed at different time points after DENA administration (Table 2). Histological examination showed that after 23 weeks of DENA treatment, the mice started developing cholangiocellular carcinoma (CCC), a rare primary carcinoma of the liver originating in bile duct cells (Fig. 1A). No HCCs were observed at that time point. HCCs were observed later after the formation of CCC, starting after 30 weeks of treatment (Fig. 1C). It is noteworthy that no liver fibrosis was observed in DENA mice (Fig. 1B).

Profiles of serum protein *N*-glycans were altered in the diethylnitrosamine mice

We analysed the serum *N*-glycan profiles in DENA-treated mice and control mice using DSA-FACE. As shown in Fig. 2, the desialylated *N*-glycan profile contained eight major peaks in control mice. No other *N*-glyans (or peaks) were found in the DENA-treated animals compared with the control animals. We performed structural analysis of the different *N*-glycans by labelling them and then treating them with exoglycosidases. This analysis showed that several *N*-glycans (such as peak 1, peak 5m and peak 6) contained a core-α-1,6-fucose structure, but did not reveal the presence of an α-1,3-fucose *N*-glycan structure (data not shown). In addition, the mouse serum *N*-glycan structures were further analysed using matrix-assisted laser desorption/ionization-time of flight mass spectrometry (MALDI-TOF MS). Here again, no α-1,3-fucose *N*-glycan or bisecting GlcNAc *N*-glycans were detected in the sera of all mice (data not shown).

We compared DENA-treated mice of the non-HCC group (with CCC but without HCC; $n = 26$) and the

Table 1. Primers used for quantitative polymerase chain reaction

	Forward (3′–5′)	Reverse (5′–3′)
Fut8	CAGGGGATTGGCGTGAAAAAG	CGTGATGGAGTTGACAACCATAG
Mgat3	ATGAAGATGAGACGCTACAAGC	GGCCAGTTCTCTCGGGAAG
Mgat4a	AAAGAGCGTCTTCGAGTGGC	ACTTCCATTAGTCTCTGCTCCA
Mgat4b	GAGGGCAGTATCCGAGAGG	CGAGACGTTCCACGGCTTC

Table 2. Development of tumours in the livers of mice given diethylnitrosamine treatment

DENA administration		Non-HCC (*n*) (cholangiocellular carcinoma)	HCC (*n*) (cholangiocellular carcinoma and HCC)
Week 23	Control mice ($n = 10$)	0	0
	DENA mice ($n = 10$)	10	0
Week 30	Control mice ($n = 8$)	0	0
	DENA mice ($n = 10$)	7	3
Week 36	Control mice ($n = 8$)	0	0
	DENA mice ($n = 12$)	8	4
Week 48	Control mice ($n = 8$)	0	0
	DENA mice ($n = 16$)	1	15

DENA, diethylnitrosamine; HCC, hepatocellular carcinoma.

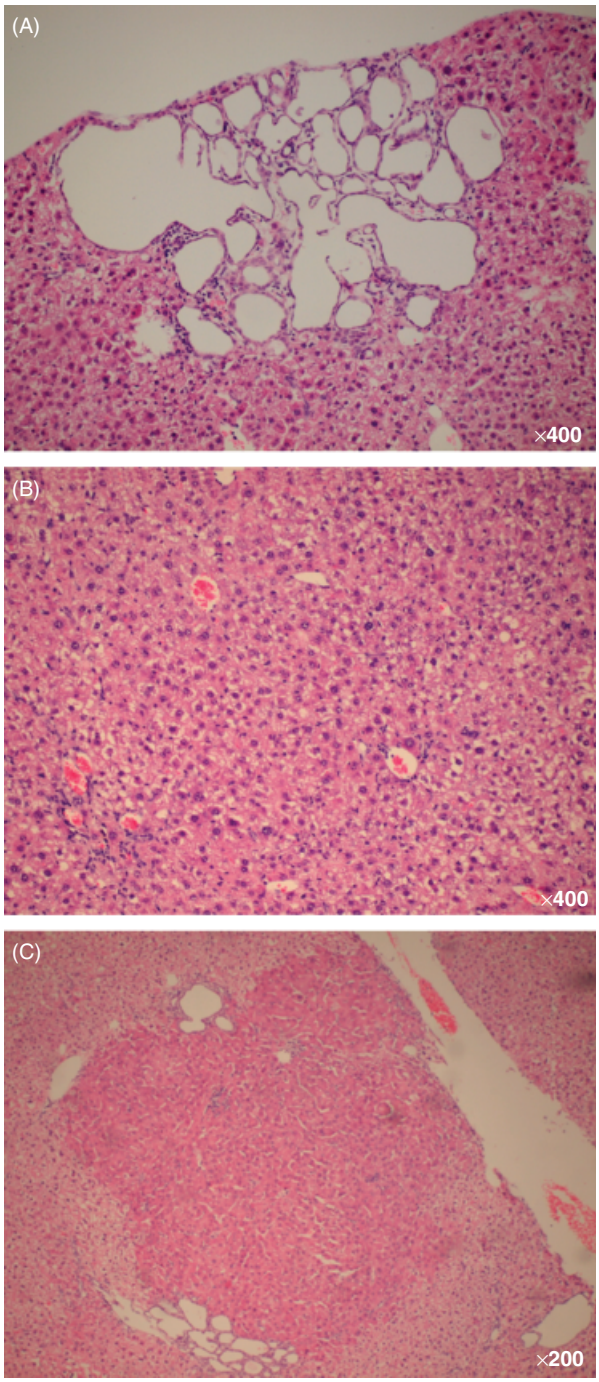

Fig. 1. Representative sections of haematoxylin and eosin-stained livers of diethylnitrosamine-treated mouse. (A) Proliferation of small bile ducts, some of which are cystically dilated. No overt signs of malignancy are present. (B) Normal liver tissue with a preserved architecture showing some portal tracts and central veins without fibrosis. (C) A relatively small HCC composed of atypical proliferation of hepatocytes.

HCC group (with both CCC and HCC; $n = 22$) with the control mice ($n = 34$). We found that peak 8 and peak 4 gradually increased but significantly ($P < 0.05$) during

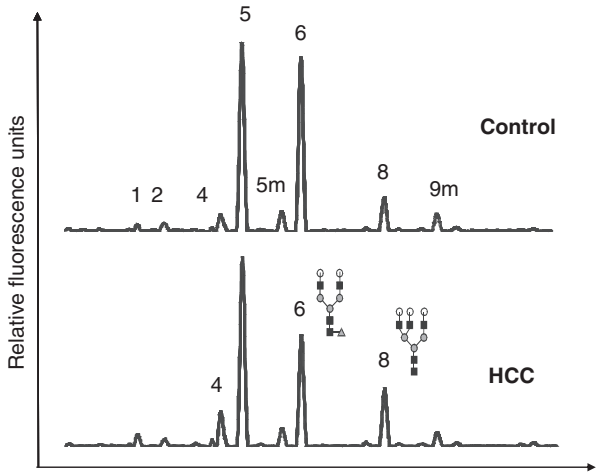

Fig. 2. Representative serum desialylated *N*-glycan profiles in C57BL/6j mouse. *N*-glycan profile from the total serum protein is showed in control mouse (the upper panel) and in DENA mouse with HCC (the lower panel). Peak 1 is an agalacto, core-α-1,6-fucosylated biantennary glycan (NGA2F), peak 5 is a bigalacto, biantennary glycan (NA2), peak 6 is a core-α-1,6-fucosylated biantennary (NA2F) and peak 8 is a tri-antennary (NA3). The structures of the *N*-glycan peak 6 and peak 8 are indicated in the lower panel. The symbols used in the structural formulas are as follows: open circle stands for β-linked galactose, square stands for β-linked *N*-acetylglucosamine (GlcNAc), filled circle stands for α/β-linked mannose and triangle stands for α-1,6-linked fucose.

the development of HCC in the treated mice (Fig. 3A and B). In contrast, peak 6 was significantly decreased ($P < 0.0001$) in the treated mice compared with the control mice, but no difference between HCC and non-HCC mice was seen (Fig. 3C).

Most serum *N*-linked glycoproteins are synthesized by the liver and B-lymphocytes. Any changes in serum total *N*-glycans could reflect alteration of liver or B-lymphocyte physiology. To find out whether the alteration of the glycan profile in total serum of DENA mice was at least partly due to changes in the *N*–glycans of immunoglobulins (mainly IgG), we examined the *N*–glycan profiles of IgG in DENA-treated mice and control mice. We purified antibodies from serum using Protein L agarose, which binds the κ light chain of all antibodies and so can interact with a wider range of Ig molecules. *N*-glycan profiles of the Ig fractions were determined by DSA-FACE. We found no alteration of Ig glycan profiles in DENA-treated mice compared with controls (data not shown), which indicates that the liver is the major source of the changes in serum glycans in DENA mice.

Regulation of *N*-glycosylation is altered in the liver of diethylnitrosamine mice

The terminal glycosylation sequences produced by the cell are presumed to reflect the expression of the corresponding glycosyltransferase. To determine whether the altered serum glycan profile in DENA mice was because

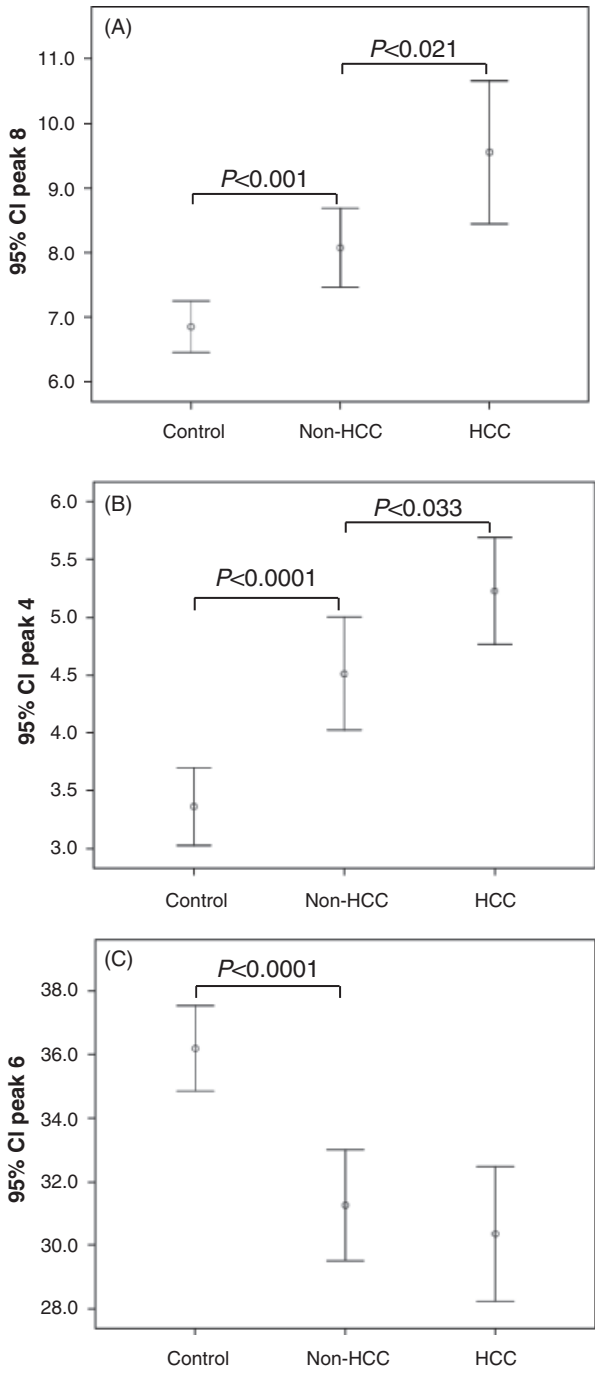

Fig. 3. Correlation of the *N*-glycan marker with the progression of hepatocellular carcinoma (HCC) in diethylnitrosamine mice. Peak 8 (A), peak 4 (B) and peak 6 (C) values plotted against the control ($n = 34$), non-HCC ($n = 26$) and HCC ($n = 22$). There was a statistically significant correlation of the three *N*-glycan values with the progress of HCC in DENA mice. The vertical axis represents the peak heights. The fit lines represent the 95% confidence interval for the mean values.

of alteration of the glycosylation biosynthesis pathway, real-time PCR was used to analyse the expression of several oligosaccharyltransferase genes in liver tissue of DENA-injected mice (HCC group and non-HCC group) and control mice.

It has been reported that α-1,6-fucosyltransferase 8 (Fut8) is the only fucosyltransferase involved in core fucosylation in mice (14). We investigated whether the decreased level of peak 6 (a core-α-1,6-fucosylated biantennary glycan) in the serum of DENA mice was caused by downregulation of Fut8 in the liver. Indeed, we found that Fut8 expression was downregulated significantly ($P < 0.0001$) in non-HCC (but with CCC) livers in DENA-treatment mice compared with control mice (Fig. 4A). The mean level of Fut8 was still lower in livers with HCC than in control livers, but the difference was not statistically significant ($P = 0.1127$) (Fig. 4B). This transcriptional regulation of Fut8 in the liver of DENA mice was correlated with the level of peak 6 in the serum, which decreased sharply in the non-HCC (but with CCC) group but was less prominent in the HCC group compared with the control mice (Fig. 3C).

Following DENA treatment, Mgat4a, which is responsible for tri-antennary glycan, Mgat4a was also significantly increased ($P < 0.001$) in the liver tissue of the non-HCC and HCC groups of DENA-treated mice (Fig. 4C and D) compared with the control mice; however, Mga4b was significantly decreased ($P < 0.0145$) in the non-HCC group, but it remained unchanged in the HCC group (Fig. 4E and F). The changes in Mgat4 might contribute to the altered concentration of peak 8 (triantennary glycan) in the serum of DENA mice.

As we mentioned above, no α-1,3-fucose *N*-glycan structures were detected in any mice sera; in agreement, expression of their corresponding genes (Fut9) was not evidenced in mouse liver (data not shown). In contrast, bisecting GlcNAc residue was not observed in both control and DENA mice sera; however, expression of Mgat3 encoding for GlcNAc TIII, which is responsible for synthesizing a bisecting GlcNAc residue, was drastically increased ($P < 0.001$) in the liver tissue of the non-HCC and HCC groups of DENA-treated mice compared with age-matched controls (Fig. 4G and H).

Discussion

Examination of liver biopsies showed that administration of DENA to C57BL/6 mice induced CCC in bile duct cells after 23 weeks and HCC after 30 weeks of treatment. We demonstrate that alteration of serum *N*-glycan profiles in mice with CCC and HCC is associated with the transcriptional regulation of glycosylation in the liver.

N-glycans are synthesized in the ER and Golgi by the subsequent addition of oligosaccharides, such as GlcNAc and fucose molecules, by the corresponding oligosaccharyltransferases (15, 16). Changes in the *N*-glycan profile in the serum could be related to changes in the expression levels of glycosyltransferases in liver cells, which would lead to modifications in both the core structures and the terminal structures of glycans (15). Indeed, we found that alterations of serum *N*-glycans in

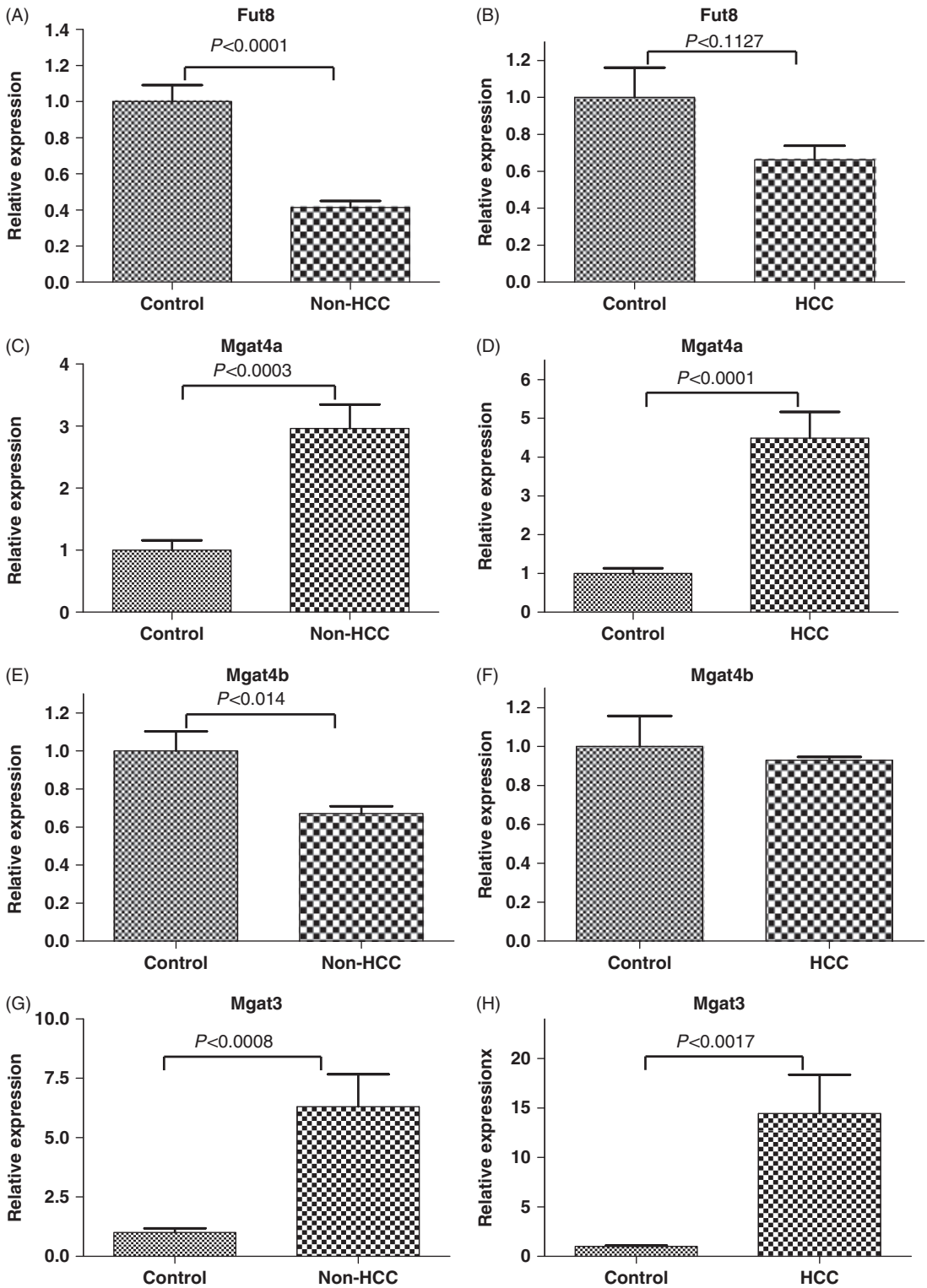

Fig. 4. Altered expression of glycosyltransferase genes in the liver of diethylnitrosamine (DENA) mice. Liver RNA was isolated from non-hepatocellular carcinoma (HCC) of DENA mice ($n = 6$) and their age-matched control mice ($n = 8$), HCC mice ($n = 6$) and their age-matched control mice ($n = 8$). Expression of the Fut8 (A, B), Mgat4a (C, D), Mgat4b (E, F) and Mgat3 (G, H) was measured by quantitative polymerase chain reaction.

DENA mice were closely correlated with the regulation of glycotransferase genes. For instance, the decreased expression of Fut8 was associated with a lower level of peak 6 (NA2F) in the serum, whereas the increased expression level of *N*-acetylglucosaminyltransferase4a was associated with a higher level of peak 8 (NA3) in the serum. However, the mechanism behind the alteration of glycosylation during HCC development is not fully understood. The function of FUT8 has been associated with transforming growth factor-β1 (TGF-β1), a potent growth inhibitor and apoptosis inducer. Signalling through the TGF-β1 receptor is downregulated in Fut8 KO mice because ligand affinity for the receptor is decreased (17). Moreover, the EGF-induced phosphorylation of EGFR was substantially blocked in Fut8 KO cells, and the binding of EGF to its receptor (EGFR) requires core fucosylation of *N*-glycans (17). EGFR is thought to be involved in the development of cancer because its gene is often amplified and/or mutated in cancer cells. It would thus be interesting to further study whether early downregulation of Fut8 in DENA mice is associated with glycosylation changes in the TGF-β1 receptor leading to reduce apoptosis on the one hand and with altered glycosylation of EGFR to suppression of the early progression of cancer on the other.

In our previous studies, the abundance of a bisecting biantennary *N*-glycan (NA2FB) and a branched α-1,3-fucosylated triantennary *N*-glycan (NA3Fb) was altered in human HCC patients with HBV infection (8). However, unlike human serum *N*-glycoproteins, the bisecting GlcNAc NA2FB and the α-1,3-fucosylated NA3Fb were detected neither by DSA-FACE nor by MALDI-TOF in mouse serum. This discrepancy can probably be explained by species-specific differences in *N*-glycosylation between humans and mice (18, 19). However, to our surprise, expression of Mgat3 (encoding GlcNAc-TIII, which synthesizes a bisecting GlcNAc residue) was drastically elevated in the liver of DENA mice. This finding is in the line with previous results showing that the expression of the Mgat3 gene is correlated with hepatic tumorigenesis in rats (20–23) and humans (24). Mice lacking GlcNAc-TIII because of mutation in *Mgat3* exhibited retarded progression of DENA-induced liver tumours (25). On the other hand, the development of DENA-induced tumours was unaltered by high levels of GlcNAc-TIII in the liver of transgenic mice, which leads to the hypothesis that retarded progression of tumours in mice lacking GlcNAc-TIII is because of the absence of the bisecting GlcNAc residue on *N*-glycans of one or more circulating glycoproteins from a tissue other than the liver (25). Although the function of *N*-acetylglucosaminyltransferase III is not clear, it has been suggested that it is involved in determining the conformation and the function of the modified proteins, including cell-surface receptors and adhesion molecules (26).

In summary, the quantitative desialylated *N*-glycan analysis system, based on DSA-FACE, is a high-throughput technology platform designed to profile *N*-glycans on proteins in the serum. Because the desialylated glycan profile is reproducible and quantitative, it is suitable for longitudinal and follow-up studies. The limitation of this method is that the sialic acid cannot be characterized because sialic acid adds an extra negative charge on the structures, which is a disadvantage in CE-based methods.

As HCC induction by DENA is an artificial model that may bear no relation to glycosylation changes that arise in human HCC, conclusions drawn from these experiments cannot be directly applied to humans. Nevertheless, we found that the levels of three *N*-glycans (peak 8, peak 4 and peak 6) changed remarkably in response to DENA treatment. To our knowledge, this is the first report on serum *N*-glycan changes during cancer progression in DENA-treated mice. The changes in serum glycans were closely correlated with cancer progression, demonstrating that they can be used to monitor the progress of HCC and to follow up treatment of liver tumours in this DENA mouse model.

Acknowledgements

We thank Dr Amin Bredan for editing the manuscript. This work was supported by a grant from Ghent University (BOF No. 01106205), Flanders-China Bilateral project (011S605).

References

1. Becker RA, Shank RC. Kinetics of formation and persistence of ethylguanines in DNA of rats and hamsters treated with diethylnitrosamine. *Cancer Res* 1985; **45**: 2076–84.
2. Lee JS, Chu IS, Mikaelyan A, *et al.* Application of comparative functional genomics to identify best-fit mouse models to study human cancer. *Nat Genet* 2004; **36**: 1306–11.
3. Jaeken J, Carchon H. Congenital disorders of glycosylation: a booming chapter of pediatrics. *Curr Opin Pediatr* 2004; **16**: 434–9.
4. Dube DH, Bertozzi CR. Glycans in cancer and inflammation–potential for therapeutics and diagnostics. *Nat Rev Drug Discov* 2005; **4**: 477–88.
5. Freeze HH, Westphal V. Balancing N-linked glycosylation to avoid disease. *Biochimie* 2001; **83**: 791–9.
6. Axford JS. Glycosylation and rheumatic disease. *Biochim Biophys Acta* 1999; **1455**: 219–29.
7. Peracaula R, Tabares G, Royle L, *et al.* Altered glycosylation pattern allows the distinction between prostate-specific antigen (PSA) from normal and tumor origins. *Glycobiology* 2003; **13**: 457–70.
8. Liu XE, Desmyter L, Gao CF, *et al.* N-glycomic changes in hepatocellular carcinoma patients with liver cirrhosis induced by hepatitis B virus. *Hepatology* 2007; **46**: 1426–35.
9. Chen C, Schmilovitz-Weiss H, Liu XE, *et al.* Serum protein N-glycans profiling for the discovery of potential biomarkers for nonalcoholic steatohepatitis. *J Proteome Res* 2009; **8**: 463–70.

10. Vanderschaeghe D, Laroy W, Sablon E, *et al*. GlycoFibroTest is a highly performant liver fibrosis biomarker derived from DNA sequencer-based serum protein glycomics. *Mol Cell Proteomics* 2009; **8**: 986–94.
11. Callewaert N, Van Vlierberghe H, Van Hecke A, *et al*. Noninvasive diagnosis of liver cirrhosis using DNA sequencer-based total serum protein glycomics. *Nat Med* 2004; **10**: 429–34.
12. Vanhooren V, Laroy W, Libert C, Chen C. N-glycan profiling in the study of human aging. *Biogerontology* 2008; **9**: 351–6.
13. Laroy W, Contreras R, Callewaert N. Glycome mapping on DNA sequencing equipment. *Nat Protoc* 2006; **1**: 397–405.
14. Wang X, Gu J, Ihara H, *et al*. Core fucosylation regulates epidermal growth factor receptor-mediated intracellular signaling. *J Biol Chem* 2006; **281**: 2572–7.
15. Dwek RA. Biological importance of glycosylation. *Dev Biol Stand* 1998; **96**: 43–7.
16. Trombetta ES, Parodi AJ. Glycoprotein reglucosylation. *Methods* 2005; **35**: 328–37.
17. Wang X, Inoue S, Gu J, *et al*. Dysregulation of TGF-beta1 receptor activation leads to abnormal lung development and emphysema-like phenotype in core fucose-deficient mice. *Proc Natl Acad Sci USA* 2005; **102**: 15791–6.
18. Hann B, Balmain A. Building 'validated' mouse models of human cancer. *Curr Opin Cell Biol* 2001; **13**: 778–84.
19. Leenders MW, Nijkamp MW, Borel Rinkes IH. Mouse models in liver cancer research: a review of current literature. *World J Gastroenterol* 2008; **14**: 6915–23.
20. Narasimhan S, Schachter H, Rajalakshmi S. Expression of N-acetylglucosaminyltransferase III in hepatic nodules during rat liver carcinogenesis promoted by orotic acid. *J Biol Chem* 1988; **263**: 1273–81.
21. Nishikawa A, Fujii S, Sugiyama T, Hayashi N, Taniguchi N. High expression of an N-acetylglucosaminyltransferase III in 3′-methyl DAB-induced hepatoma and ascites hepatoma. *Biochem Biophys Res Commun* 1988; **152**: 107–12.
22. Nishikawa A, Gu J, Fujii S, Taniguchi N. Determination of N-acetylglucosaminyltransferases III, IV and V in normal and hepatoma tissues of rats. *Biochim Biophys Acta* 1990; **1035**: 313–8.
23. Miyoshi E, Nishikawa A, Ihara Y, *et al*. N-acetylglucosaminyltransferase III and V messenger RNA levels in LEC rats during hepatocarcinogenesis. *Cancer Res* 1993; **53**: 3899–902.
24. Mori S, Aoyagi Y, Yanagi M, Suzuki Y, Asakura H. Serum N-acetylglucosaminyltransferase III activities in hepatocellular carcinoma. *J Gastroenterol Hepatol* 1998; **13**: 610–9.
25. Yang X, Bhaumik M, Bhattacharyya R, *et al*. New evidence for an extra-hepatic role of N-acetylglucosaminyltransferase III in the progression of diethylnitrosamine-induced liver tumors in mice. *Cancer Res* 2000; **60**: 3313–9.
26. Takahashi M, Kuroki Y, Ohtsubo K, Taniguchi N. Core fucose and bisecting GlcNAc, the direct modifiers of the N-glycan core: their functions and target proteins. *Carbohydr Res* 2009; **344**: 1387–90.